International Journal of Nanomedicine

Dovepress
open access to scientific and medical research

Open Access Full Text Article

ORIGINAL RESEARCH

3D printed zirconia ceramic hip joint with precise structure and broad-spectrum antibacterial properties

This article was published in the following Dove Press journal:
International Journal of Nanomedicine

Yanglong Zhu[1]
Kuan Liu[2]
Jianjian Deng[1]
Jing Ye[1]
Fanrong Ai[3]
Huan Ouyang[4]
Tianlong Wu[1]
Jingyu Jia[1]
Xigao Cheng[1]
Xiaolei Wang[2]

[1]Department of Orthopedic Surgery, The Second Affiliated Hospital of Nanchang University, Nanchang 330006, People's Republic of China; [2]Institute of Translational Medicine, Nanchang University, Nanchang 330088, People's Republic of China; [3]School of Mechanical & Electronic Engineering, Nanchang University, Nanchang 330031, People's Republic of China; [4]Department of Vascular Surgery, The Second Affiliated Hospital of Nanchang University, Nanchang 330006, People's Republic of China

Correspondence: Xigao Cheng
Department of Orthopedic Surgery, The Second Affiliated Hospital of Nanchang University, Nanchang 330006, People's Republic of China
Tel +861 387 061 5428
Email 228206846@qq.com

Xiaolei Wang
Institute of Translational Medicine, Nanchang University, Chinese Academy of Sciences, 1299 Xuefu Road, Tan New District Nanchang, Honggu 330031, People's Republic of China
Tel +861 867 985 0415
Email wangxiaolei@ncu.edu.cn

Background: Nowadays, zirconia ceramic implants are widely used as a kind of hip prosthesis material because of their excellent biocompatibility and long-term wear resistance. However, the hip joint is one of the major joints with complex 3D morphological structure and greatly individual differences, which usually causes great material waste during the process of surgical selection of prosthesis.

Methods: In this paper, by combining ceramic 3D printing technology with antibacterial nano-modification, zirconia ceramic implant material was obtained with precise 3D structure and effective antibacterial properties. Among which, two technical problems (fragile and sintering induced irregular shrinkage) of 3D printed ceramics were effectively minimized by optimizing the reaction conditions and selective area inversing compensation. Through in vivo and in vitro experiments, it was confirmed that the as prepared hip prosthesis could precisely matched the corresponding parts, which also exhibited good biocompatibility and impressive antibacterial activities.

Results: 1) Two inherent technical problems (fragile and sintering induced irregular shrinkage) of 3D printed ceramics were effectively minimized by optimizing the reaction conditions and selective area inversing compensation. 2) It could be seen that the surface of the ZrO_2 material was covered with a layer of ZnO nano-particles. A universal testing machine was used to measure the tensile, bending and compression experiments of ceramic samples. It could be found that the proposed ZnO modification had no significant effect on the mechanical properties of ZrO_2 ceramics. 3) According to the plate counting results, ceramics modified with ZnO exhibited significantly higher antibacterial efficiency than pure ZrO_2 ceramics, the ZrO_2-ZnO ceramics had a significant killing effect 8 hours. 4) The removed implants and the tissue surrounding the implant were subjected to HE staining. For ZrO_2-ZnO ceramics, inflammation was slight, while for pure ZrO_2 ceramics, the inflammatory response could be seen that the antibacterial rate of the ZrO_2-ZnO ceramics was significantly better than that of the pure ZrO_2 ceramics group. 5) It could be seen that the cytotoxicity did not increase proportionally with the increase of concentration, all of viability were still above 80%. This suggested that our materials were safe and could be applied as a type of potential biomaterial in the future. 6) Further animal studies demonstrated that the implant was in good position without dislocation. This resulted implied that the proposed method can achieve accurate 3D printing preparation of ceramic joints. In addition, the femurs and surrounding muscles around the implant were then sectioned and HE stained. Results of muscle tissue sections further showed no significant tissue abnormalities, and the growth of new bone tissue was observed in the sections of bone tissue.

Conclusion: 1) The ceramic 3D printing technology combined with antibacterial nano-modification can quickly customize the ideal implant material with precise structure, wear-

submit your manuscript | www.dovepress.com
DovePress
http://doi.org/10.2147/IJN.S202457

resistant and effective antibacterial properties. 2) Two inherent technical problems (fragile and sintering induced irregular shrinkage) of 3D printed ceramics were effectively minimized by optimizing the reaction conditions and selective area inversing compensation. 3) ZnO nano-materials were modified on the ceramic surface, which could effectively killing pathogenic bacteria.

Keywords: zirconia, 3D printing, antibacterial, surface modification, implant material

Introduction

With the prolongation of life expectancy, especially the occurrence of various traffic accidents and sports injuries, the number of arthroplasty operations is increasing steadily every year. Taking hip replacement surgery as an example, more than 600,000 people need hip replacement surgery every year.[1] And it is estimated that this number will exceed 1 million by 2030.[1] At present, the materials applied to the hip prosthesis are mainly metals represented by titanium.[2] This kind of metal material generally has a service life of less than 20 years. Due to the limited wear resistance, the long-term use of titanium-based implants will result in the emergence of metal grinding particles,[3] which would cause inflammation around the surrounding tissue. This inevitable phenomenon can eventually lead to the failure of total hip arthroplasty and require reoperation, which causes physical pain and financial burden to the patients.[4]

Compared with metal materials, bioceramic material is a promising alternative implant, which can significantly reduce the wear rate of implants.[5,6] For instance, the 3 mol % yttria partially stabilized tetragonal zirconia is a typical ceramic material with excellent mechanical properties, which has great application prospects in orthopedics.[7] At the same time, the zirconium oxide (ZrO_2) ceramics, with good corrosion resistance, are potentially alternative materials that can meet the requirements of long-term usage. For example, Lohmann et al[8] in 2002 and Manicone et al[9] in 2007 proved that ZrO_2 has good biocompatibility. Vagkopoulou[10] in 2009 confirmed the excellent mechanical properties of ZrO_2 ceramic. These reports had contributed greatly to the improvement of the physical properties and biocompatibility of ceramic hip joint materials. However, the hip joint[11] is one of the major joints with complex three-dimensional (3D) morphological structure and great individual differences. The precise matching degree between the shape of the prosthesis and the corresponding site of the patient is thus an important factor that affects the use experience after operation. At present, during the procedures of the actual surgery, hospitals always need to prepare several spare prostheses for doctors to choose, which results in a great waste of materials (Figure S1). These non-customized prostheses are still difficult to accurately match the patients' actual hip 3D structures. Moreover, the procedures for selecting suitable prosthesis during operation also intangibly the time of operation, which increases the amount of intraoperative blood loss and the risk of infection. In addition, ZrO_2 ceramics do not have obvious antibacterial properties. Therefore, one of the core research aims in the development of customized implant is how to realize precisely 3D construction of ZrO_2 ceramic implant materials with certain antibacterial properties.[12]

Theoretically, with the aid of the current clinical imaging technology, it is possible to provide the precise 3D structural date of the implant prosthesis before surgery. Afterward by combining ceramic 3D printing technology[13–15] with antibacterial nanomodification[16–18] (Figure 1), it is possible to quickly customize an ideal implant material with precise 3D structure and effective antibacterial properties. However, after the ceramic joint precursor is prepared by 3D printing technology, the subsequent polymerization and sintering steps are still needed, both of which would lead to the shrinkage or even fracture of the ceramic joint. As a result, the obtained implant is difficult to precisely match the surgical site. Based on the above information, the purpose of this study is to solve the above two technical problems (fragile and irregular shrinkage) of 3D ceramic implant printing. The rabbits' femur was selected as the animal model system.

Experimental section

Material preparation

A commercially available high purity 3 mol% yttria partially stabilized zirconium oxide (3Y-ZrO_2)[19,20] was used as a raw material. An aqueous solution of a mixture of 3Y-ZrO_2 nanopowder and ammonium citrate (dispersant) was used for the preparation of the slurry. The pH of the solution was adjusted to about 9 by using 2% ammonia.

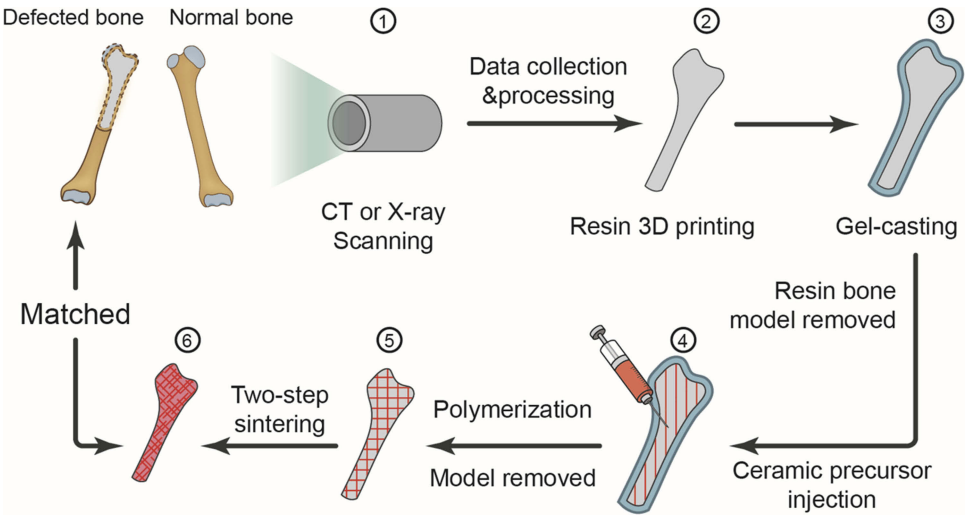

Figure 1 Illustration of the ceramic hip joint prosthesis fabrication processes by gel-casting method combined with 3D printing technology.

Then, acrylamide (monomer), N,N'-methylene bisacrylamide (crosslinking agent), ammonium persulfate (initiator) and tetramethylethyl enediamine (catalyst) were sequentially added. The ceramic slurry was fully stirred until no bubbles formed.

Fabrication of the implant

The implants with precise matching structure can be customized by the method of gel-casting molding combined with 3D printing technology. Figure 1 shows the whole fabrication process of pure ZrO_2 ceramic joint. First, the rabbits' hip joint was scanned by CT or X-ray to obtain 3D data of 3D structures, and the resulting data was printed by a 3D printer (Makerbot Z18, America) to produce a resin hip prosthesis. Then, the hip joint mold was cast by gel-casting method, and the ceramic precursor materials were injected into the mold, and the mold of the injected material was kept under the humidity of 50% and placed in a vacuum environment of 55°C for gelation and drying for 2 days. Finally, the pure ZrO_2 ceramic hip prosthesis with precisely matched structure could be obtained by sintering.

Two-step sintering

The dried samples were sintered by the method of a two-step sintering. Firstly, the heating rate was 2°C/min to 1,000°C, and the temperature was kept at this temperature for 10 hrs. Then, the heating rate was 20°C/min to 1,200°C, and the temperature was kept at this temperature for 2 hrs. Finally, 3Y-ZrO_2 ceramics were obtained by cooling in furnace.[21]

Fabrication of ZnO layered modified ceramics

Zinc oxide solution (ZnO)[22] was obtained by adding 50 mM $Zn(NO_3)_2 \cdot 6H_2O$, 80 mM $NH_3 \cdot H_2O$ and 25 mM hexamine into 400 mL deionized water in 85°C water bath for 24 hrs. Then, the zinc oxide solution was sucked onto the surface of ceramics to form ZnO modified ceramics (ZrO_2-ZnO).[23]

Mechanical properties

The synthetic ceramic slurry was slowly poured into a 3D printed molds to form two different shapes of ceramics: rod-shaped ceramics and columnar ceramics. The synthetic rod-shaped ceramics were used in tensile tests and bending tests, and the columnar ceramics were used in compression tests. A universal testing machine was used to measure the tensile, bending and compression experiments of ceramic samples at the loading rate of 0.01 mm/s. Each group was measured three times repeatedly.

In vitro antibacterial properties assay

Two bacteria, *Escherichia coli* (*E. coli*, ATCC 25922) and *Staphylococcus aureus* (*S. aureus*, ATCC 25923), the most common clinical orthopedic infections, were selected to evaluate the antibacterial ability of ZnO samples. The surface unmodified ceramics were used as a control group, and all samples were sterilized with ethylene oxide before the experiments. *E. coli* and *S. aureus* were cultured at 37°C for 24 hrs and adjusted to a concentration of 10^7 CFU/mL. Then, 100 μL of the bacterial stock solution was added to 5 mL of Luria–Bertani broth, with

control group, ZrO_2 nanomaterials, and ZrO_2–ZnO nanomaterials. The culture was carried out for 8 hrs in an orbital shaker. Each sample was ultrasonic (100 W) for 2 s. After that, 100 μL cocultured medium was diluted to 10^5 CFU/mL, and 50 μL dilution solution was coated to the culture dish and then placed in a constant temperature incubator for 24 hrs. The antibacterial effects of the three groups of samples were compared by plate counting method. The antibacterial rate (R) of *E. coli* and *S. aureus* in the medium was calculated based on the following formula: R=(A - B)/A ×100%, where A stands for the number of bacteria in the control group and B means the number of bacteria in the experimental group.[24]

In vivo antibacterial tests and histological analysis

In this experiment, 12 male rats (Sprague−Dawley) weighing between 224 g and 263 g (8 weeks old, Animal Science department of Jiangxi Province) were used to evaluate the inflammatory response with *S. aureus* of the ZrO_2 nanomaterials and ZrO_2–ZnO nanomaterials after implantation in vivo. The operations were performed by two experimenters under standard aseptic conditions. Preoperatively, the rats were fasted for 24 hrs besides drinking water without limitation. Rats were continuously fed 2 hrs after the operation. Rats were anesthetized by intraperitoneal injection of 3.6% chloral hydrate (1 mL per 100 g). The dorsal hair portion of each rat was shaved, sterilized, and created a 1.5–2 cm midline incision. Using sharp and blunt dissection, we formed a subcutaneous sac under the incision. The sterilized under layer implants of ZrO_2–ZnO ceramics for four rats and pure ZrO_2 ceramics for four rats. The ceramics (pure ZrO_2, ZrO_2-ZnO) soaked with physiological saline (0.9% NaCl) were implanted under the skin. Later, subcutaneous tissues were injected with 0.2 mL of a bacterial suspension of *S. aureus* ATCC 25923 at 10^4 CFU/mL. After surgery, the back incisions were closed with sutures and the rats were injected subcutaneously with normal saline (1−2 mL/g) for rehydration.

After waking up, the mice were paired in cages and moved unrestricted. Two weeks after the operation, the rats were euthanized with carbon dioxide asphyxiation. The implant material and surrounding tissue, including adjacent skin, were removed and placed in 5 mL of physiologic saline. After sonication, the solution was used for bacterial quantification. Then, 100 μL cocultured medium was taken out for 10^4 degrees of dilution, and 50 μL of the dilution solution was coated on the culture dish and then placed in a constant temperature incubator (37°C) for 24 hrs. The antibacterial activity of the samples was compared by plate counting method. The collected samples were fixed with 10% neutralizing buffer formalin for 24 hrs. After standard treatment, the fixed specimens were placed in paraffin and sectioned longitudinally with a microtome (5 μm thickness). The sections were stained with HE for optical microscopy examination.

Cytotoxicity assay

The cytotoxicity of the ZrO_2–ZnO materials was analyzed by cell counting kit-8 (CCK-8) assay. The cytotoxicity tests were carried out by indirect contact method. The extract was prepared according to the ratio of 1.25 cm^2/mL in ISO 10993, and the final concentration gradient was set to 1.25, 0.625, 0.3125, 0.15625, and 0.078125 cm^2/mL when the cells were cultured. First, a cell suspension was prepared: MC3T3-E1 cells in a good growth state and in logarithmic growth phase were counted. Cell culture conditions were complete medium (90% α-MEM +10% FBS +1% PS, purchased from Gibco), at 37°C and 5% CO_2 incubator. The above cell suspension was inoculated into a 96-well plate, and the number of cells inoculated was 1,000 cells/well; the cells were cultured in incubator set at 37°C for 6 hrs, and after the cells were attached, the medium was replaced with dilute material extract according to the grouping and time points. Only the complete medium was added to the blank control group. When the cells were grown for 1, 3 and 7 days, the medium containing 10% CCK-8 (Japan Dongren Chemical) was directly placed for replacement. Incubation was carried out for 1 hr at 37°C, and the absorbance at 450 nm was measured by a microplate reader (Bio-Tek).

In vivo biocompatibility studies

Six New Zealand white rabbits (2.5–3.0 kg) were used to observe their biocompatibility in vivo. The surgery was performed by two experimenters under standard aseptic conditions. Rabbits were anesthetized with 10% chloral hydrate (3 mL/kg). The rabbits' legs were shaved, washed, and sterilized with iodine. After the start of the operation, the skin incision, blunt separation of the muscles and the femur were revealed. The ceramic hip prosthesis was sterilized and implanted into rabbits. The surgical sites were stratified closed; the muscle, fascia and internal dermis were sutured with 4–0 Vicryl and the outer dermis

were sutured with 3–0 Vicryl. The animals were monitored for any possible complications during the recovery and given free access to water and rabbit food during the healing period.

Four weeks after implantation, the animals were euthanized and the implants were exposed by sharp separation to the bones. The bones adjacent to the implant were then removed together with the muscles and stored in 10% formalin for further histological analysis. The paraffin-embedded tissues were cut into 5-mm serial sections and stained with the conventional HE method.

Statistical analysis

Results were expressed as the mean ± standard deviation, and the data were statistically analyzed by one-way ANOVA, followed by multiple SD comparisons among groups using the LSD (L) and Tukey HSD posthoc test and (IBM SPSS Statistics, version 23.0). The data were considered to be significantly different when p levels of 0.05, 0.01 and 0.001 were obtained.

Results and discussion

The methods of solving two technical problems (fragile and irregular shrinkage)

Theoretically, the above two technical problems could be solved through optimizing reaction condition and selective area inversing compensation. First, Figure 2A shows the rabbit hip joint, which was divided into six regions, namely, A, greater trochanter area; B, trochanter tertius area; C, distal end of the femoral shaft area; D, center of femoral shaft area; E, caput femoris area; F, edge of femoral shaft area. Figure 2B is a shrinkage ratio illustration of a 1.3 times magnified rabbit hip joint ceramic prosthesis prepared by gel-casting along with 3D printing technology. The red arrow refers to the size of the rabbit hip joint ceramic prosthesis before sintering, the blue arrow refers to the size of rabbit hip joint ceramic prosthesis after sintering and the dashed line represents the actual size of the rabbit hip joint required. As a result, this 1.3 times magnified ceramic hip prosthesis, after shrinkage, was still smaller than the actual rabbit hip joint anatomical size. Therefore, the size of the implant

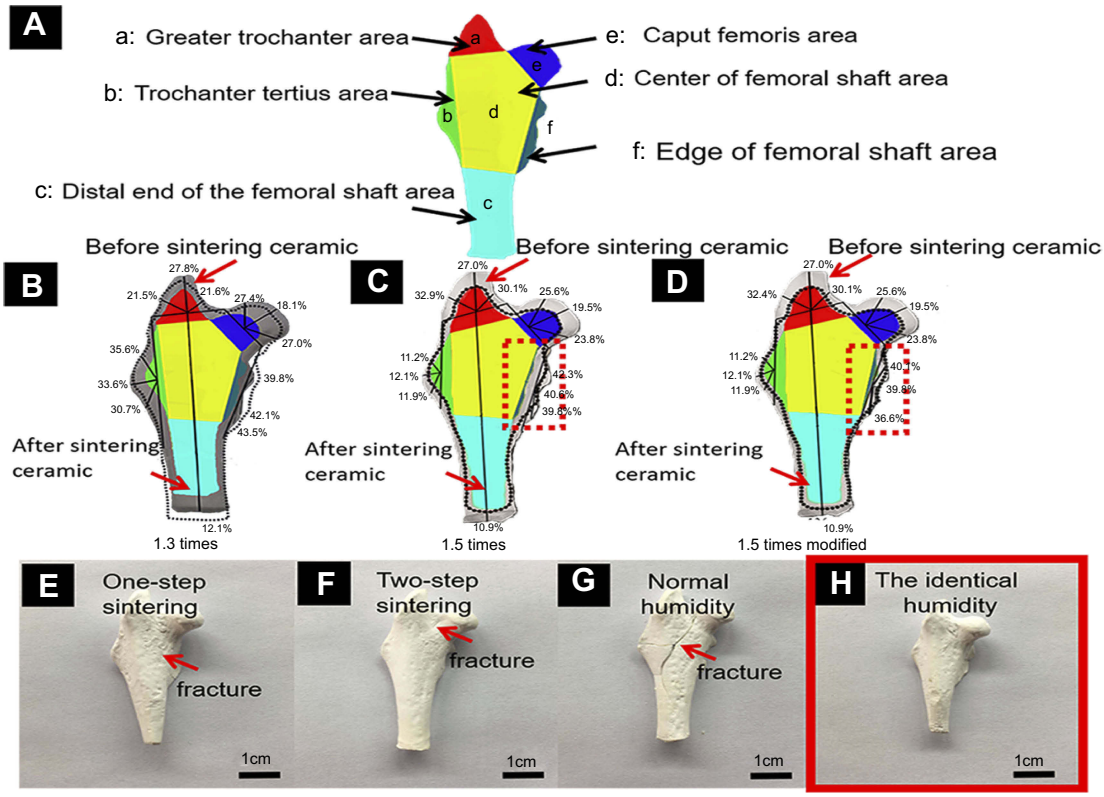

Figure 2 The six partitions of the rabbit hip joint (**A**). Shrinkage ratio diagram of a rabbit hip joint ceramic prosthesis with a 1.3 times magnification before sintering (**B**). Shrinkage ratio diagram of a rabbit hip joint ceramic prosthesis with a 1.5 times magnification before sintering (**C**). Shrinkage ratio diagram of a revised rabbit hip joint ceramic prosthesis with a 1.5 times magnification as well as some special area (f area) modification parameters of the ceramic prosthesis (**D**). Optical images of ceramic prosthesis made by conventional one-step sintering method (**E**); by two-step sintering method (**F**); polymerized under normal humidity conditions (**G**); polymerized under a constant humidity conditions (**H**) respectively.

should be further increased before sintering. Figure 2C shows a 1.5 times magnified rabbit hip joint ceramic prosthesis. It could be found that most areas were basically in accordance with the rabbit hip joint anatomical size after sintering. However, the F area was still smaller than the rabbit hip joint anatomical size. We also concluded that the closer to the central region (D), the greater the proportion of contraction would occur. Figure 2D shows a magnified 1.5 times rabbit hip joint ceramic prosthesis made by further improving the 3D printing parameters (F area was further enlarged 20% particularly). It could be found that after sintering, the regions after the contraction basically conform to the rabbit hip joint anatomical size.

Afterward, aiming at the problem of different degrees of fracture after the polymerization and sintering of ceramic hip prosthesis, we then systematically optimize the reaction conditions of ZrO_2 ceramics. Figure 2E shows a rabbit hip joint ceramic prosthesis made by a conventional one-step sintering method. The red arrow marked the area of the fractures. Figure 2F shows a ceramic prosthesis produced by a two-step sintering method. As a result, fractures were still observed. Figure 2G shows a ceramic prosthesis that was polymerized under normal humidity conditions, and fractures still exhibited after sintering. Figure 2H shows a ceramic prosthesis that was polymerized under the conditions with identical humidity (50%). After sintering, a flawless ceramic hip prosthesis could be obtained. Through the above research, it could be found that the method of fixed humidity of 50% and selective area inversing compensation could effectively solve the two typical technical problems of ceramic 3D printing after sintering.

The characterization of pure ZrO_2 and ZnO_2–ZnO

In order to improve the antibacterial properties, nano-ZnO modification was introduced in this work. Figure 3A shows a pure ZrO_2 ceramic hip prosthesis customized by gel-casting method combined with 3D printing technology. Figure 3B shows the microstructure of pure ZrO_2 ceramic obtained by SEM after sintering. It could be seen that the ZrO_2 particles were tightly bonded together. Figure 3C is the energy spectrum data of pure ZrO_2 ceramics. Figure 3D displays a ZrO_2–ZnO ceramic hip prosthesis. Figure 3E shows the

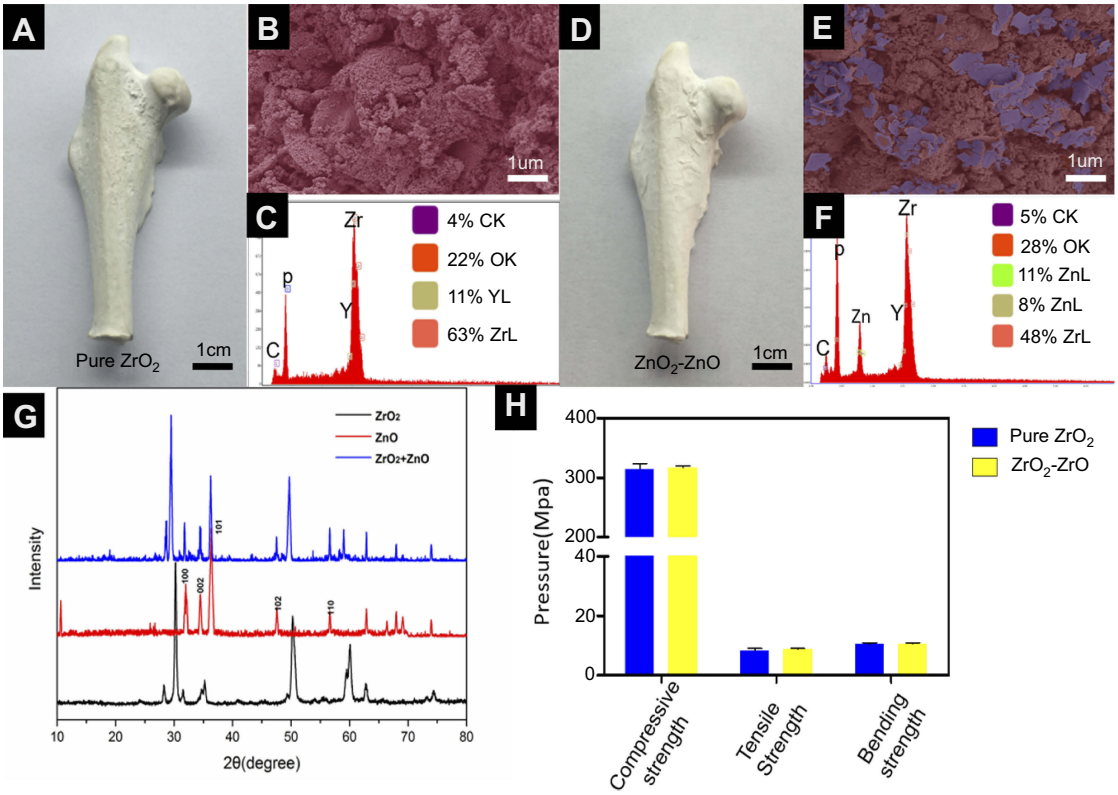

Figure 3 Optical images of material samples (**A**) Pure ZrO_2; (**D**) ZrO_2-ZnO. SEM pictures of material samples (**B**) Pure ZrO_2; (**E**) ZrO_2-ZnO. Photograph of material sample by electron microscope (**C**) Pure ZrO_2; (**F**) ZrO_2-ZnO. XRD Spectra of three different materials (**G**). Mechanical properties of two kinds of materials (**H**).

microstructure of ZrO_2–ZnO ceramic after sintering. It could be seen that the surface of the ZrO_2 material was covered with a layer of ZnO nanoparticles. Figure 3F shows the energy spectrum data of ZrO_2–ZnO ceramics, and it could be seen that the Zn element had been added to the material. Figure 3G illustrates the XRD of pure ZrO_2 ceramic, ZnO nanomaterials and ZrO_2–ZnO ceramic, respectively. The presence of ZnO absorption peaks could be seen in ZrO_2–ZnO ceramics. These results indicated that we had successfully modified ZnO on the surface of pure ZrO_2 ceramics. Figure 3H represents the mechanical properties of pure ZrO_2 ceramics and ZrO_2–ZnO ceramics. It could be found that ZnO had no significant effect on the mechanical properties of ZrO_2 ceramics.

Antibacterial properties and cytotoxicity

As shown in Figure 4, we tested the antibacterial properties of pure ZrO_2 ceramics and ZrO_2–ZnO ceramics. The pure ZrO_2 ceramics, with no obvious antibacterial property, were selected as the control group. *E. coli* and *S. aureus* were used in the experiment. These two types of bacteria were the most common pathogen in clinical practice. According to the plate counting results from Figure 4A, ceramics modified with ZnO exhibited significantly higher antibacterial efficiency than pure ZrO_2 ceramics. As shown in Figure 4B, the ZrO_2–ZnO ceramics had a significant killing effect after 8 hrs (Gram-negative antibacterial rate was 91.7±1.1%, Gram-positive antibacterial rate was 99.8±0.25%). The above results indicated that the ZrO_2–ZnO ceramics had a fast and broad-spectrum bactericidal property. We then carried out in vivo experiments to verify the antibacterial properties of this material. The preparation of pure ZrO_2 ceramics and ZrO_2–ZnO ceramics was sterilized before implanted. Afterward, *S. aureus* were injected into the implant area after the surgery. Two weeks later, we removed these implants as well as the tissue surrounding the implants. It could be seen from Figure 4C and D that the

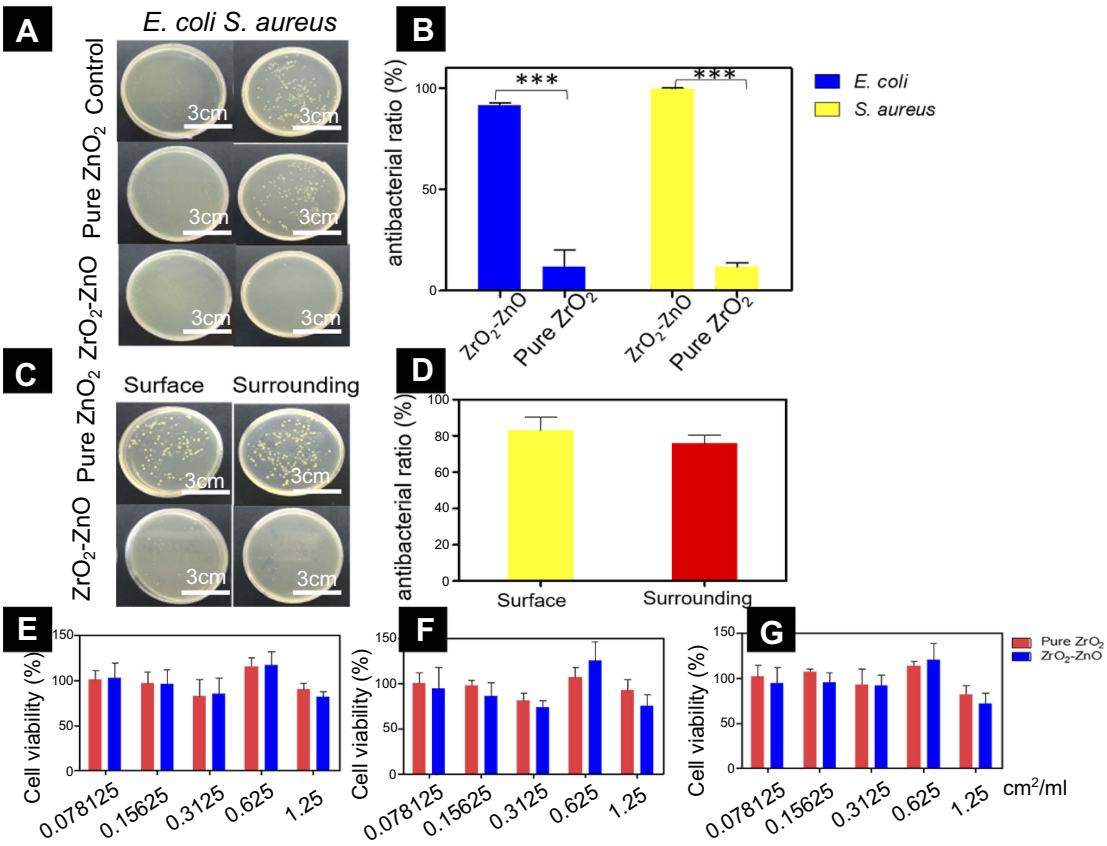

Figure 4 The plate counting results of Pure ZrO_2 and ZrO_2-ZnO against *S. aureus* and *E. coli* in vitro (**A**). Antibacterial studies of Pure ZrO_2 and ZrO_2-ZnO against *S. aureus* and *E.coli* in vitro (**B**). 2 weeks after implantation in the body, the plate counting results for bacteria on the surface of the implants and surrounding tissue (**C**). Antibacterial activity of the Pure ZrO_2 and ZrO_2-ZnO on the surface and surrounding, 2 weeks after surgery (**D**). The cell viability of different groups of materials after co-culture with osteoblasts for 1 day (**E**), 3 days (**F**), and 7 days (**G**). *p< 0.05, **p< 0.01, ***p< 0.001. Data were averaged from at least three tests. Error bars show standard deviations.

antibacterial rate of the ZrO_2–ZnO ceramics was significantly better than that of the pure ZrO_2 ceramics group.

Although ZrO_2 ceramics modified by zinc oxide nanomaterials had excellent antibacterial properties, its biocompatibility was also very important. Therefore, we then carried out cytotoxicity tests by using the osteoblasts. Figure 4E–G shows the viability of cells cultured at different concentrations of extract after 1, 3 and 7 days. It could be seen that the cytotoxicity did not increase proportionally with the increase of concentration, all of the viability were still above 80%. The ZrO_2–ZnO ceramics had slight cytotoxicity, but the cell survival rate was still above 80%. This suggested that our materials were safe and could be applied as a type of potential biomaterial in the future.

Animal experiments

The removed implants and the tissue surrounding the implant were then subjected to HE staining. As shown in Figure 5A–D,

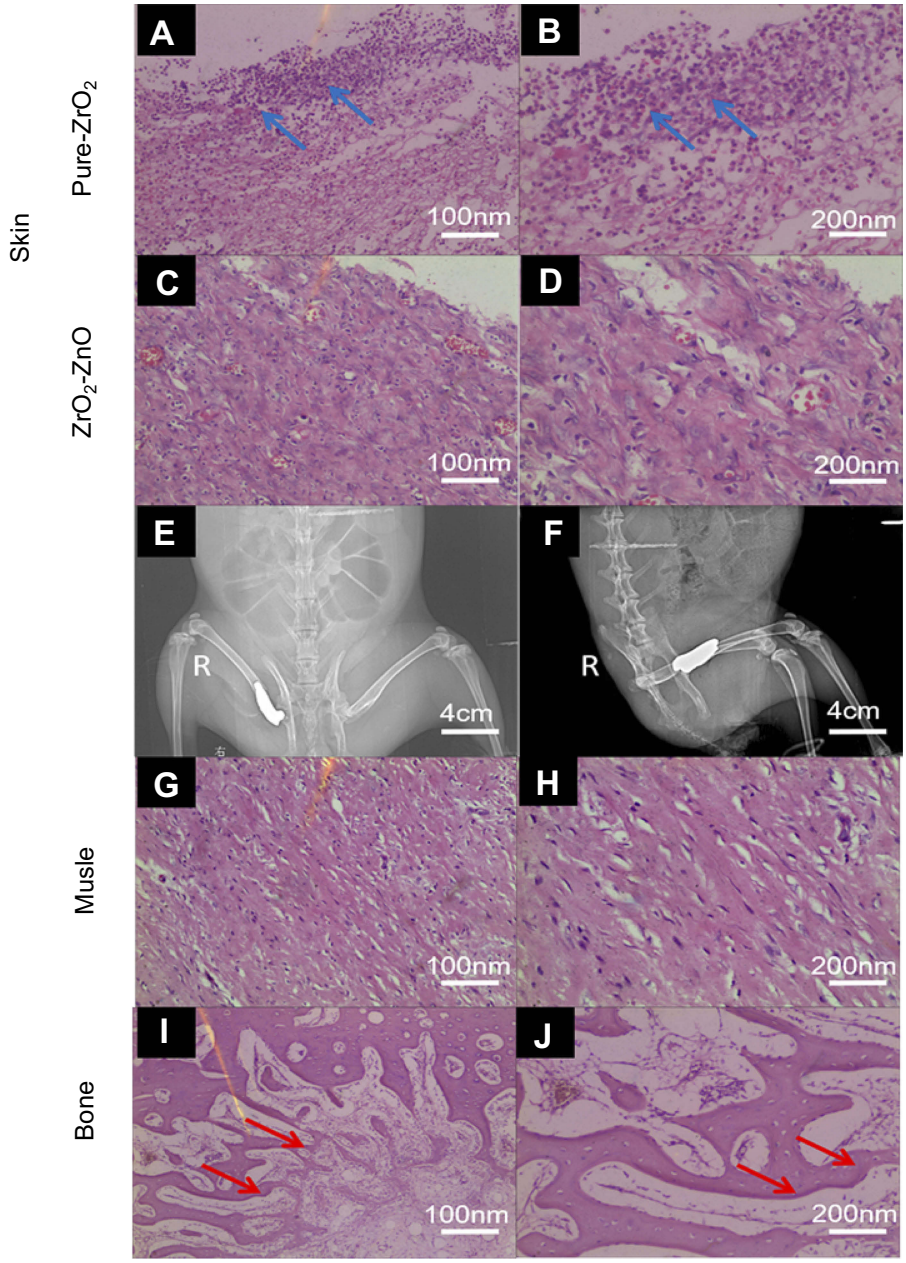

Figure 5 2 weeks after co-cultured with *S. aureus* in vivo, the tissues around the implant materials were stained by the HE staining. (**A**, **B**) come from pure ZrO_2 ceramic; (**C**, **D**) come from ZrO_2-ZnO ceramic, the direction of the blue arrow was inflammatory cells. X-ray diffraction patterns of the ZrO_2-ZnO ceramic hip prosthesis after implantation (**E**, **F**). After 4 weeks of in vivo biocompatibility experiments, surrounding tissues (bone and muscle) around the implant were removed for HE staining to examine (**G**, **H**) muscle and (**I**, **J**) bone area.

for ZrO_2–ZnO ceramics, inflammation was slight (as compared with the negative control group), while for pure ZrO_2 ceramics, the inflammatory response was remarkably serious.

Figure 5E and F shows the positive lateral radiographs of the ceramic hip prosthesis implanted in vivo. It could be seen that the implant was in a good position without dislocation. This result implied that the proposed method can indeed achieve accurate 3D printing preparation of ceramic joints. In addition, the femurs and surrounding muscles around the implant were then sectioned and HE stained. Results from Figure 5G and H showed that muscle tissue sections further showed no significant tissue abnormalities, and the growth of new bone tissue was seen in the sections of bone tissue (Figure 5I and J). All the results showed that the ZrO_2–ZnO ceramics had good biocompatibility when contacting bone tissue and surrounding muscle tissue.

Conclusions

In theory, the ceramic 3D printing technology combined with antibacterial nanomodification can quickly customize the ideal implant material with precise structure, wear-resistant and effective antibacterial properties. However, in the process of actual operation, the ceramic joint shrinkage and fracture occur during the preparation of ceramic joint precursor material. In order to overcome these two disadvantages, we optimized the reaction conditions and introduced a selective area inversing compensation strategy. Moreover, in this experiment, we added ZnO nanomaterials to the ceramic surface, which could effectively kill pathogenic bacteria. The current work can provide some theoretical bases and technical support for future customized 3D printing ceramic joints. It should be noted that brittleness is another key issue that limits the wide application of ceramics.[25] Further research on the brittleness of ceramics is also needed before further clinical applications.

Ethical statement

Mice were purchased from Animal Center of Nanchang University (Nanchang, China). The animals were maintained in a room temperature (20–22°C) and 40–50% humidity. Mice were provided with water and a 12 hr light/dark cycle. All animal procedures were performed according to protocols approved by the Institutional Animal Care and Use Committee at Institute of Translational Medicine, Nanchang University (no. 2016NC-020-02) and animal handling followed the dictates of the National Animal Welfare Law of China. The research has been approved by the Bioethics Committee of Translational Medicine of Nanchang University (permission No. YK/92/2016).

Acknowledgments

This work was supported by the National Natural Science Foundation of China (No. 31860263 to Xiaolei Wang; No. 81660357 and 81860397 to Xigao Cheng); Science Foundation of Jiangxi Provincial Department of Education (20165BCB19002, KJLD14010 20153BCB23035 and 20161ACB21002 to Xiaolei Wang).

Disclosure

The authors report no conflicts of interest in this work.

References

1. Kurtz S, Ong K, Lau E, Mowat F, Halpern M. Projections of primary and revision hip and knee arthroplasty in the United States from 2005 to 2030. *J Bone Joint Surg Am*. 2007;89:780–785.
2. Lewallen EA, Riester SM, Bonin CA, et al. Biological strategies for improved osseointegration and osteoinduction of porous metal orthopedic implants. *Tissue Eng Part B Rev*. 2015;21:218–230. doi:10.1089/ten.teb.2014.0333
3. Passuti N, Philippeau J, Gouin F. Friction couples in total hip replacement. *Orthop Traumatol Surg Res*. 2009;95:27–34. doi:10.1016/j.otsr.2009.04.003
4. Langton DJ, Jameson SS, Joyce TJ, Hallab NJ, Natu S, Nargol AV. Early failure of metal-on-metal bearings in hip resurfacing and large-diameter total hip replacement. *J Bone Joint Surg Br*. 2010;92:38–46. doi:10.1302/0301-620X.92B1.22770
5. Chevalier J. What future for zirconia as a biomaterial? *Biomaterials*. 2006;27:535–543. doi:10.1016/j.biomaterials.2005.07.034
6. Jiang L, Liao Y, Wan Q, Li W. Effects of sintering temperature and particle size on the translucency of zirconium dioxide dental ceramic. *J Mater Sci Mater Med*. 2011;22:2429–2435. doi:10.1007/s10856-011-4403-7
7. Scarano A, Di CF, Quaranta M, Piattelli A. Bone response to zirconia ceramic implants: an experimental study in rabbits. *J Oral Implantol*. 2003;29:8–12. doi:10.1563/1548-1336(2003)029<0008:BRTZCI>2.3.CO;2
8. Lohmann CH, Dean DD, Köster G, et al. Ceramic and PMMA particles differentially affect osteoblast phenotype. *Biomaterials*. 2002;23:1855–1863. doi:10.1016/S0142-9612(01)00312-X
9. Manicone PF, Rossi IP, Raffaelli L. An overview of zirconia ceramics: basic properties and clinical applications. *J Dent*. 2007;35:819–826. doi:10.1016/j.jdent.2007.07.008
10. Vagkopoulou T, Koutayas SO, Koidis P, Strub JR. Zirconia in dentistry: part 1. Discovering the nature of an upcoming bioceramic. *Eur J Esthet Dent*. 2009;4:130–151.
11. Roy T, Choudhury D, Ghosh S, Mamat AB, Pingguan-Murphy B. Improved friction and wear performance of micro dimpled ceramic-on-ceramic interface for hip joint arthroplasty. *Ceram Int*. 2015;41:681–690. doi:10.1016/j.ceramint.2014.08.123
12. Wei T, Yu Q, Zhan W, Chen H. A smart antibacterial surface for the on-demand killing and releasing of bacteria. *Adv Healthc Mater*. 2016;5:449–456. doi:10.1002/adhm.201500700
13. Placone JK, Engler AJ. Recent advances in extrusion-based 3D printing for biomedical applications. *Adv Healthc Mater*. 2018;7:e1701161. doi:10.1002/adhm.201701161

14. Richards DJ, Tan Y, Jia J, Yao H, Mei Y. Isr. 3D printing for tissue engineering. *J Chem*. 2013;53:805–814.
15. Do AV, Khorsand B, Geary SM, Salem AK. 3D printing of scaffolds for tissue regeneration applications. *Adv Healthc Mater*. 2015;4:1742–1762. doi:10.1002/adhm.201500168
16. Wang X, Yang F, Yang W, Yang X. A study on the antibacterial activity of one-dimensional ZnO nanowire arrays: effects of the orientation and plane surface. *Chem Commun (Camb)*. 2007;14:4419–4421. doi:10.1039/b708662h
17. Wang X, Zhu H, Yang F, Yang X. Biofilm-engineered nanostructures. *Adv Mater Weinheim*. 2010;21:2815–2818. doi:10.1002/adma.200802598
18. Yu F, Fang X, Jia H, et al. Zn or O? An atomic level comparison on antibacterial activities of zinc oxides. *Chemistry*. 2016;22:8053–8058. doi:10.1002/chem.201601018
19. Gutierrez MI, Penilla EH, Leija L, Vera A, Garay JE, Aguilar G. Novel cranial implants of yttria-stabilized zirconia as acoustic windows for ultrasonic brain therapy. *Adv Healthc Mater*. 2017;21:1700214. doi:10.1007/s10856-011-4403-7
20. Acuña LM, Lamas DG, Fuentes RO, et al. Local atomic structure in tetragonal pure ZrO_2 nanopowders. *J Appl Crystallogr*. 2010;43:227–236. doi:10.1107/S0021889809054983
21. Manosso MK, Chinelatto AL. Two-steps sintering of alumina-zirconia ceramics. *Mater Sci Forum*. 2010;600–601:819–825. doi:10.4028/www.scientific.net/MSF.660-661.819
22. Podrezova LV, Cauda V, Stassi S, Cicero G, Abdullin KA, Alpysbaeva BE. Properties of ZnO nanorods grown by hydrothermal synthesis on conductive layers. *Cryst Res Tech*. 2015;49:599–605. doi:10.1002/crat.201300372
23. Hang L, Miao X, Jing Y, et al. Falling leaves inspired ZnO nanorods −nanoslices hierarchical structure for implant surface modification with two stage releasing features. *ACS Appl Mater Interfaces*. 2017;9:13009–13015. doi:10.1021/acsami.7b00666
24. Miao X, Liao H, Deng Z, et al. "Dandelion" inspired dual-layered nanoarrays with two model releasing features for the surface modification of 3D printing implants. *ACS Biomater Sci Eng*. 2017;3:2259–2266. doi:10.1021/acsbiomaterials.7b00456
25. Li C, Ai F, Miao X, et al. "The return of ceramic implants": rose stem inspired dual layered modification of ceramic scaffolds with improved mechanical and anti-infective properties. *Mater Sci Eng C Mater Biol Appl*. 2018;93:873–879. doi:10.1016/j.msec.2018.07.063

Supplementary materials

Chemicals and reagents:

3 mol% yttria partially stabilized zirconium oxide (3Y-ZrO_2) were purchased from haitai Co, Ltd. (Shanghai, China). Ammonium citrate, Ammonium persulphate (APS), Acrylamide (AM), and N,N'-methylene diacrylamide (MBAM) was purchased from Macklin Reagent Technologies Co, Ltd. (ShangHai, China). N,N,N',N'-Tetramethylethylenediamine was purchased from Hope Bio-Technology Co, Ltd. (ShanDong, China). The Cell counting kit-8 (CCK-8) were purchased from Solarbio Co, Ltd. (Beijing, China).

Characterization:

The field-emission scanning electron microscope (FE-SEM) (Zeiss, Germany) was used to examine the surface morphologies of the sample. The crystal structure of the sample was determined by X-ray diffraction (XD-3, Germany).

Figure S1 During the procedures of actual surgery, hospitals always need to prepare several spare prostheses for doctors to choose. The red arrow referred to the hip joint prostheses.